



Coordinated operation of pumped-storage hydropower with power and water distribution systems

November 2022

Changing the World's Energy Future

Majid Majidi, Masood Parvania, Luis Rodriguez-Garcia, Thomas M Mosier



DISCLAIMER

This information was prepared as an account of work sponsored by an agency of the U.S. Government. Neither the U.S. Government nor any agency thereof, nor any of their employees, makes any warranty, expressed or implied, or assumes any legal liability or responsibility for the accuracy, completeness, or usefulness, of any information, apparatus, product, or process disclosed, or represents that its use would not infringe privately owned rights. References herein to any specific commercial product, process, or service by trade name, trade mark, manufacturer, or otherwise, does not necessarily constitute or imply its endorsement, recommendation, or favoring by the U.S. Government or any agency thereof. The views and opinions of authors expressed herein do not necessarily state or reflect those of the U.S. Government or any agency thereof.

Coordinated operation of pumped-storage hydropower with power and water distribution systems

Majid Majidi, Masood Parvania, Luis Rodriguez-Garcia, Thomas M Mosier

November 2022

**Idaho National Laboratory
Idaho Falls, Idaho 83415**

<http://www.inl.gov>

**Prepared for the
U.S. Department of Energy
Under DOE Idaho Operations Office
Contract DE-AC07-05ID14517**

Coordinated Operation of Pumped-Storage Hydropower with Power and Water Distribution Systems

M. Majidi^a, L. Rodriguez-Garcia^a, T. M. Mosier^b, M. Parvania^{a,*}

^a*Department of Electrical and Computer Engineering, University of Utah*

^b*Power and Energy Systems Department, Idaho National Laboratory*

Abstract

Small pumped-storage hydropower (PSH) units have gained popularity as distributed energy storage options that can provide flexibility to the operation of power distribution systems. Optimal operation of small PSH units is not only dependent on the energy storage provided to power distribution system, but also on the inflow and outflow of water from and to the water distribution system. In this context, this paper develops an optimization model for coordinated operation of PSH units with power and water distribution systems. The proposed model optimizes the operation of water tanks, variable-speed pumps and PSH in pumping and generating modes to minimize the operation cost of power distribution system, while respecting the power flow constraints of power distribution and hydraulic constraints of water distribution system. Appropriate electricity tariffs are implemented to avoid additional expenses in water distribution system that can be enforced by its coordinated operation in favor of power distribution system. The proposed model is implemented on a 33-bus and a 123-bus test power distribution system connected to a 16-node test water distribution system. Results demonstrate the effectiveness of proposed model in tapping PSH flexibility to reduce the operation cost of power and water distribution systems, while meeting the power and water demands.

Keywords: Pumped-storage hydropower, coordinated operation, power distribution system, water distribution system

*Corresponding author

Email addresses: majid.majidi@utah.edu (M. Majidi), luis.rodriguez@utah.edu (L. Rodriguez-Garcia), thomas.mosier@inl.gov (T. M. Mosier), masood.parvania@utah.edu (M. Parvania)

Preprint submitted to International Journal of Electrical Power & Energy Systems March 20, 2023

1. Introduction

1.1. Problem Definition and Background

The interdependence of power and water infrastructure provides opportunities for enhancing the operational performance of both systems [1]. Coordinated operation of power and water systems, i.e., power distribution systems (PDSs) and water distribution systems (WDSs) provides the decision-makers in both systems with financial cost-savings, while ensuring reliable delivery of power and water to the consumers [2, 3]. The main idea to coordinate the operation of interdependent power and water systems is to tap the flexibility of existing energy units, and leverage both systems' operations such that the cost of supplying energy is minimized and physical constraints in the operating systems are satisfied [4, 5, 6].

Benefits of incorporating flexible energy units such as variable-speed pumps and water tanks in coordinated operation of water systems have been explored in multiple research studies [2, 3, 4, 5, 6]. In addition to the mentioned flexible energy units, great efforts are recently made to assess how distributed hydropower generation units can add to the efficiency of water systems and leverage their coordination with power systems. These units can use flexibility in the water system (e.g., through reservoirs) to support power system operation, as stored water can help to reduce the power consumption of pumps at peak hours [7]. Moreover, in-conduit hydropower generation offers an alternative for power generation from the energy in the water flow of existing tunnels, canals, and pipelines. One way to add in-conduit hydropower generation to the existing power and water distribution infrastructures is to develop and model small-scale pumped-storage hydropower (PSH) that can utilize both pumps and hydropower generation devices to offer energy efficiency for the operating systems [8].

Based on the desired technology, PSH units can be designed for different applications [9]. In some cases, PSH units are specifically designed and constructed to offer charge/discharge services, while for others, the existing pump stations in water systems are converted to operate as PSH units, which can supply the water network requirements while generating electricity [10]. For instance, in [11], pump as turbine (PAT) is developed to enable charge/discharge of energy in a combined heat and power system and increase the system efficiency when supplying a variety of loads, e.g., electricity load,

heat load, water load, etc. PAT is employed in [12] to offer energy recovery and pressure control services to WDS operation, concerning the economic convenience and system flexibility.

PSH units are usually constructed in larger scales, but their application is being extended to small distributed PSH units that are designed for micro applications, concerning their lower environmental impact and functionalities in balancing power grids [13]. In [14], PAT is employed as a solution to increase energy efficiency in a small-scale microgrid with on-site renewable generation sources. In [15], feasibility of integrating small PSH in buildings is investigated and parameters associated with the design of PSH are determined. Small PSH units offer an alternative energy storage mechanism to enable the integration of DERs in power systems. These units can share some of the existing infrastructure from the WDS, such as reservoir capacity and pipes, thereby reducing cost of the technology [8]. This potential co-development and associated co-operation can also be applied to remote power-water systems, such as municipal water systems for remote communities or irrigation systems. These systems typically require extensive pumping, providing significant electricity load. Small PSH units can potentially couple with these systems to shift load, store excess electricity when loads are low and support peak electricity requirements [16]. Small PSH can also support integration of renewable energy resources by improving the flexibility of operating portions of the grid in islanded mode or supporting grid operation in rural or remote areas that have significant variable renewable generation. In [17], an energy management scheme is developed for a small-scale islanded microgrid, where different combinations of renewable sources such as photovoltaic (PV) unit, wind turbine and small PSH are studied to determine the optimal techno-economic performance of the microgrid. The authors in [18, 19] developed optimization schemes to determine the optimal energy supply settings for remote and isolated communities, where the capabilities of PV units, wind turbines, hydropower turbines and small PSH units in supplying reliable and cost-efficient energy to the communities are assessed.

In rural areas, in order to supply water for different applications, such as irrigation and public supply, renewable generation is used to pump water into specific reservoirs and at the times of need, the stored water with sufficient pressure head is used for energy generation along with satisfying the water demand. This application of PSH is reflected in [20], where a renewable hybrid system integrated with PAT is developed to optimize energy efficiency in supplying power and water requirements of an isolated village. Application

of PSH to continuous power generation in hybrid systems is also investigated in [21, 22], where hybrid energy systems consisting of wind unit and PSH are developed to enable local power generation in rural areas, while securing the voltage level. The results showed that optimal operation of PSH unit with different levels of wind generation can provide the community with constant electricity generation and voltage level.

As discussed, technical literature includes several valuable studies regarding the benefits introduced by PSH integration to the operation of energy complexes, especially in remote areas. In most of these studies [9]-[22], PSH is utilized to offer charge/discharge services and mitigate the uncertainty in renewable generation, thus increasing efficiency in supplying energy to the local communities. The merits of applying coordination schemes to the joint operation of power and water distribution systems are highlighted in multiple literature studies [2, 3]. These studies focused on the development of coordination frameworks for joint operation of power and water distribution systems, taking into account the flexibility introduced by variable-speed pumps, water tanks, water desalination and treatment plants. The results of these studies showed that coordination schemes can contribute to the reduction of operation cost in power and water distribution systems. Similar coordination frameworks are also presented for large-scale power and water systems in [4]-[6], where it is shown that the flexibility added by the operation of water pumps and tanks to power system provides economic revenues and cost-saving opportunities in supplying power and water load requirements.

To the best of our knowledge, the studies in [2]-[6] do not consider the role of small PSH as an additional source of flexibility in joint operation of power and water distribution systems. As small-scale PSH devices are proven to be effective in increasing energy efficiency of interdependent power and water systems, adding such flexible sources into power and water distribution systems, which already benefit from water tanks and pumping facilities, can provide the operating systems with further efficiency and cost-savings in supplying power and water load requirements. Therefore, the most beneficial way to integrate small-scale PSH units and tap their potentials in coordinated/uncoordinated operation of power and water distribution systems still needs to be explored. To do this, an efficient mathematical-based approach is required to not only integrate small PSH and handle the complexity in modeling energy flows within power and water distribution systems but also determine the optimal level of charge/discharge service deliverable by small PSH to the operation of both systems.

1.2. Contribution and Paper Structure

This paper develops an optimization model to integrate small PSH into coordinated operation of power and water distribution systems. The proposed model optimizes the coordinated operation of small PSH as an energy storage mechanism to provide the desired energy flexibility for the PDS, while respecting the water input/output flow of PSH from/to WDS and serving the power and water requirements of both systems. Compared to the existing coordination models for power and water distribution systems in the literature, the proposed model takes advantage of the small PSH to further leverage the WDS operation and accordingly provide energy flexibility to the operation of both power and water distribution systems. More specifically, the proposed coordination model takes into account the power flow constraints in PDS and dynamic technical factors in WDS operation, i.e., pressure head difference between the tank and WDS connection nodes and water flow within the WDS pipes, and coordinates the small PSH operation with the operation of power and water distribution systems, in order to minimize the day-ahead operation cost of PDS, while meeting power and water demands in both operating systems. Multiple cases capture in detail the effective role of small PSH to provide considerable amount of energy flexibility and reduce the operation cost in power and water distribution systems.

The structure of the proposed model for integrating small PSH into power and water distribution systems operation is depicted in Fig. 1. In this model, the PDS operator seeks to economically supply the energy requirements in PDS based on the upstream grid price and energy demand forecasts, and the operational constraints of both power and water distribution systems involved in supplying power and water demands. The proposed model takes into account the inherent interdependence between power and water distribution systems established by PSH in both pumping and generation modes, as well as by pumping stations and water storage tanks. Also, by implementing a dynamic electricity tariff scheme, the proposed model avoids enforcement of additional expenses to the coordinated operation of WDS, thus minimizing energy consumption cost in this system.

In the proposed model, PDS operation is modeled as a second-order cone programming problem and the power balance constraints are modeled using Branch Flow formulation. Due to the non-linearity of hydraulic constraints, WDS operation is a non-linear model. Therefore, by applying mixed-integer linear formulation, non-linear terms in the operation of WDS integrated with small PSH are linearized and the ultimate operation optimization model is

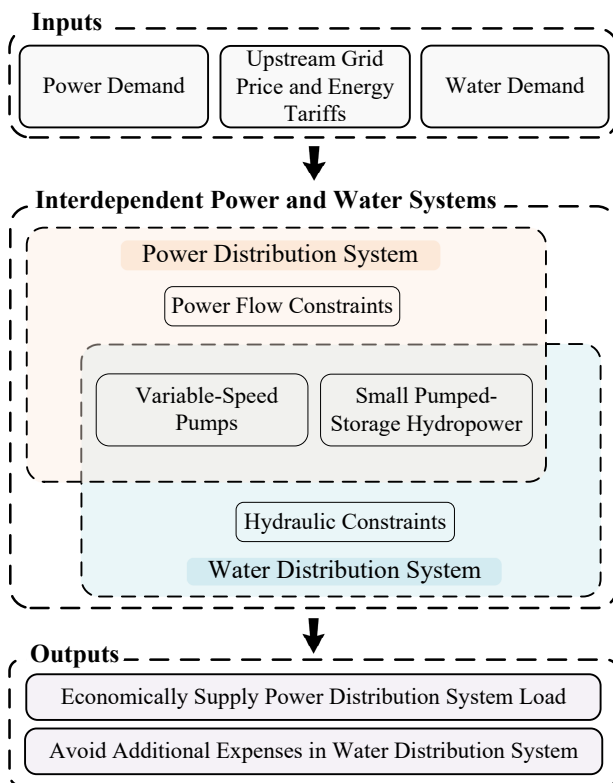


Figure 1: Structure of the proposed coordination model for power and water distribution systems with small pumped-storage hydropower unit.

formulated as a mixed-integer second-order cone programming (MISOCP) problem, solvable by commercial solvers, e.g., CPLEX.

The rest of this paper is organized as follows: The architecture and operation model of small PSH units and its integration with the operation of power and water distribution systems is presented in Section 2. The formulation of the proposed optimization model for PSH operation in interdependent power and water distribution systems is presented in Section 3. Numerical results of the proposed model are presented for a test 33-bus and a 123-bus PDS and 16-node WDS in Section 4, and conclusions are drawn in Section 5.

2. Small Pumped-Storage Hydropower Unit

This section presents the operational features of small PSH unit and the modeling considerations for its integration into the operation of power and

water distribution systems. A PSH unit acts as a coupling mechanism between power and water systems, which interacts with both systems to leverage the potential of their interdependent operation. The small PSH unit model developed in this paper is conceived to be controllable in order to provide flexibility from the power system power consumption while ensuring the water system operating conditions.

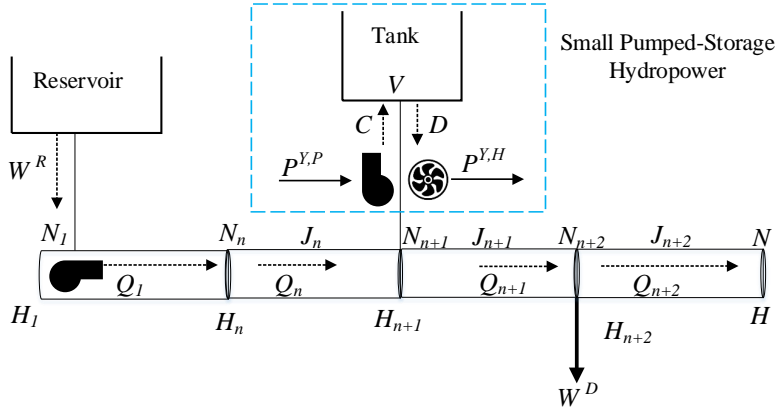


Figure 2: Interdependence of pumped-storage hydropower with power and water distribution systems.

The PSH unit is modeled and integrated into power and water distribution systems operation as depicted in Fig. 2. The PSH unit is composed of a finite capacity tank for water storage, which is connected to one of the nodes in the WDS for water exchange with the pipeline interconnection. The water is conveyed from the connection node to the tank by means of a variable-speed pump with a controllable flow rate according to the pump specifications. Once stored, water can be discharged back into the WDS, depending on the water supply and power generation requirements. Initially, the discharged water flow is used to drive the small PSH unit turbine for power generation, to then be supplied in the connection water node. The resulting power extracted from the water flow is injected as a distributed energy resource to the PDS.

The operation of small PSH tank, pump, and turbine, along with the charging and discharging flows must satisfy the WDS hydraulic constraints, which are further detailed in Section 3. On the other hand, since the pumping and generation processes involved in the operation of small PSH units are extended into the power system, new terms associated with the small PSH

power consumption/generation are introduced in the power balance equations of PDS operation. The power required for PSH pumping operation, $P^{Y,P}$, is calculated as a function of the head rise $\Delta H^{Y,P}$ and the charging flow C :

$$P^{Y,P} = \frac{\rho g \Delta H^{Y,P} C}{\eta^P}, \quad (1)$$

where ρ is the water density; g is the gravity and η^P is the pump efficiency. Similarly, the power generation obtained from the PSH unit discharge $P^{Y,H}$ is a function of the available head $H^{Y,H}$, which corresponds to the difference between the tank head and the WDS connection node head, and the discharge flow from the tank to the WDS, D :

$$P^{Y,H} = \eta^H \rho g H^{Y,H} D, \quad (2)$$

where η^H is the generator efficiency. The PSH unit intensifies the interdependency between power and water distribution systems caused by the pumping and treatment process in the water system operation. Nonetheless, the operating modes of the PSH unit lead to benefits on each system and extended into the other. The water discharged into the WDS increases the pressure head at the connection node, reducing the pump electricity consumption. At the same time, the water allocation offers an alternative for energy storage to compensate for the power demand during PDS peak load hours. In that case, the inclusion of water storage offers an opportunity to allocate resources, while taking advantage of the electricity price variations, reducing costs, and satisfying the operational constraints of both systems. This exhibits the potential of PSH unit for the interdependent operation of power and water distribution systems, where the energy efficiency introduced by this unit leverages flexible operation of both systems to reduce the cost of supplied energy to the consumers.

3. Problem Formulation

This section introduces the proposed optimization model to integrate the small PSH unit into the interdependent operation of power and water distribution systems. The objective function of the proposed model, expressed in (3), aims at minimizing the daily operation cost of PDS, which depends on the cost of electricity transacted from the transmission system and the cost

of electricity supplied from the small PSH units over the scheduling horizon of NT periods.

$$\min \sum_{t=1}^{NT} \left(P_t^{DN} \times \lambda_t^{LMP} + \sum_{y=1}^Y P_{y,t}^{Y,H} \times \lambda_t^{FIT} \right). \quad (3)$$

The first term in (3) is the cost of purchasing power P_t^{DN} from the upstream transmission system at the price of λ_t^{LMP} at time t . The second term in (3) is the cost of power purchased from small PSH units, where $P_{y,t}^{Y,H}$ is the generated power by small PSH y at time t ; Y is the total number of PSH units in the integrated operation of power and water distribution systems and λ_t^{FIT} is the discharging price of small PSH to PDS at time t , calculated based on the feed-in tariff in PDS. The objective function (3) is subject to the operating constraints of both power and water distribution systems, which are described next.

3.1. Power Distribution System Constraints

In this part, the operational constraints associated with the PDS operation are presented. The PDS model formulated in (4)-(11) uses the Branch Flow formulation to represent the active and reactive power balances, considering the power required by pumps, power injection from the PSH, as well as the voltage and flow limits within the distribution system [23].

3.1.1. Power Balance Constraints

The power balance is applied to substation (bus 1) and feeder buses, where the variables in each case are shown in Fig. 3. Based on Fig. 3, the active and reactive power flow constraints at the substation bus in the PDS are expressed in (4)-(5), where Q_t^{DN} is the reactive power taken from the upstream transmission network; $P_{1k,t}^F$ and $Q_{1k,t}^F$ are the active and reactive power flows from the substation bus to the bus k at time t ; $V_{1,t}^{sq}$ is the squared bus voltage at time t ; \mathcal{L} is the set of power lines; g_1 and b_1 stand for the shunt conductance and susceptance connected at the substation bus, respectively.

$$P_t^{DN} = \sum_{1k \in \mathcal{L}} P_{1k,t}^F + g_1 V_{1,t}^{sq}, \quad \forall t, \quad (4)$$

$$Q_t^{DN} = \sum_{1k \in \mathcal{L}} Q_{1k,t}^F + b_1 V_{1,t}^{sq}, \quad \forall t. \quad (5)$$

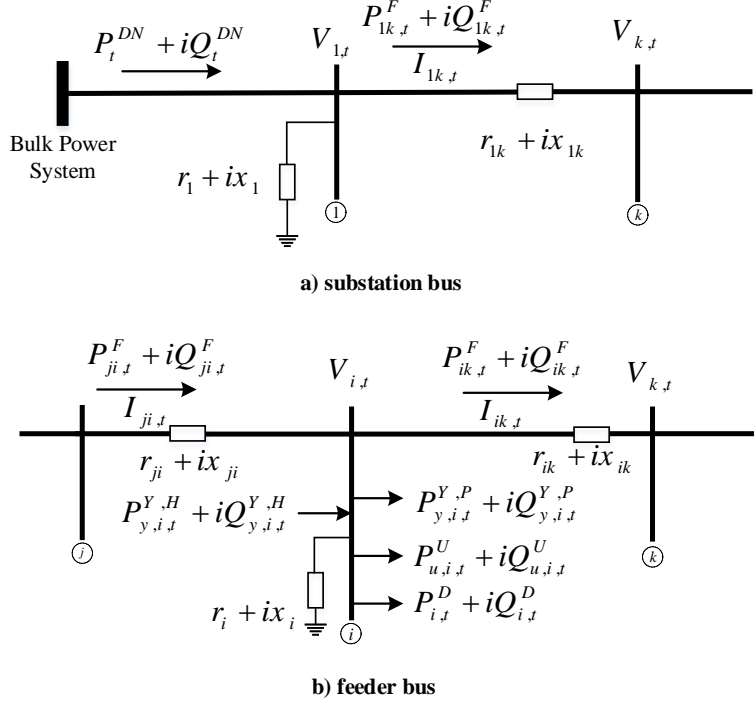


Figure 3: Power balance for Branch Flow Model formulation.

The active and reactive power balance constraints for the other buses in the PDS are expressed in (6)-(7), where load requirements including the electricity demand in the PDS and power requirement of pumps in the WDS are met by the power flows from other buses and small PSH. In (6)-(7), $P_{ik,t}^F$ and $Q_{ik,t}^F$ are the active and reactive power flows from bus i to the bus k at time t ; $P_{ji,t}^F$ and $Q_{ji,t}^F$ are the active and reactive power flows from bus j to the bus i at time t ; r_{ji} and x_{ji} are respectively the resistance and reactance of the line connecting bus j to the bus i ; $P_{i,t}^D$ and $Q_{i,t}^D$ are the active and reactive loads at bus i and time t ; $P_{u,i,t}^U$, $Q_{u,i,t}^U$ are the active and reactive power consumptions of pump u in the WDS connected to the bus i at time t ; \mathcal{U}_i is the set to map pump u to the bus i ; $P_{y,i,t}^{Y,P}$, $P_{y,i,t}^{Y,H}$ are the active power consumption and injection of small PSH y into bus i at time t ; \mathcal{Y}_i is the set to map PSH unit y to the bus i ; $Q_{y,i,t}^{Y,P}$, $Q_{y,i,t}^{Y,H}$ are the reactive power consumption and injection of small PSH y into bus i at time t ; $I_{ji,t}^{sq}$ is the squared current flow from bus j to the bus i at time t ; g_i , b_i stand for the shunt conductance

and susceptance connected to the bus i and \mathcal{B} is the set of buses.

$$P_{ik,t}^F + P_{i,t}^D + \sum_{u \in \mathcal{U}_i} P_{u,i,t}^U + \sum_{y \in \mathcal{Y}_i} P_{y,i,t}^{Y,P} = \sum_{y \in \mathcal{Y}_i} P_{y,i,t}^{Y,H} + \sum_{ji \in \mathcal{L}} (P_{ji,t}^F - r_{ji} I_{ji,t}^{sq}) + g_i V_{i,t}^{sq}, \quad \forall i \in \mathcal{B}, \forall t, \quad (6)$$

$$Q_{ik,t}^F + Q_{i,t}^D + \sum_{u \in \mathcal{U}_i} Q_{u,i,t}^U + \sum_{y \in \mathcal{Y}_i} Q_{y,i,t}^{Y,P} = \sum_{y \in \mathcal{Y}_i} Q_{y,i,t}^{Y,H} + \sum_{ji \in \mathcal{L}} (Q_{ji,t}^F - x_{ji} I_{ji,t}^{sq}) + b_i V_{i,t}^{sq}, \quad \forall i \in \mathcal{B}, \forall t. \quad (7)$$

3.1.2. Technical Constraints

The voltage drop constraint in the PDS is modeled in (8) and voltage limits on each bus are applied in (9), where \underline{V}_i^{sq} and \overline{V}_i^{sq} are the squared lower and upper limits of voltage magnitude. Current flow in the PDS is limited in (10), where \overline{I}_{ji} is the squared rated current flow of the line connecting bus j to the bus i . Complex power flows of the lines are limited in the inequality constraint (11) that represents a convex form of the original equality constraint $V_{i,t}^{sq} I_{ji,t}^{sq} = P_{ji,t}^2 + Q_{ji,t}^2$ [23].

$$V_{i,t}^{sq} - V_{j,t}^{sq} = -2 (r_{ji} P_{ji,t}^F + x_{ji} Q_{ji,t}^F) + (r_{ji}^2 + x_{ji}^2) I_{ji,t}^{sq}, \quad \forall (ji) \in \mathcal{L}, \forall t, \quad (8)$$

$$\underline{V}_i^{sq} \leq V_{i,t}^{sq} \leq \overline{V}_i^{sq}, \quad \forall i \in \mathcal{B}, \forall t, \quad (9)$$

$$I_{ji,t}^{sq} \leq \overline{I}_{ji}^2, \quad \forall (ji) \in \mathcal{L}, \forall t, \quad (10)$$

$$V_{i,t}^{sq} I_{ji,t}^{sq} \geq P_{ji,t}^2 + Q_{ji,t}^2, \quad \forall (ji) \in \mathcal{L}, \forall t. \quad (11)$$

In order to capture the flexibility introduced by coordinated operation of WDS with small PSH to the PDS operation, formulated in (4)-(11), the interdependence between power and water distribution system operation, as well as the hydraulic constraints in the WDS should be also taken into account. We describe the interdependence model next and then formulate the WDS operation.

3.2. Interdependence in Power and Water Distribution Systems

Here we briefly describe the way interdependent power and water distribution systems are connected. In Fig. 3, water pump u and PSH unit y are connected to the bus i and seek to be served as electricity loads in the PDS, where $P_{u,i,t}^U$ and $P_{y,i,t}^{Y,P}$ stand for the pumping power of pump u and PSH y , respectively. On the other side, when operating in the discharging mode, PSH unit y is considered as a source of electricity supply for PDS operation, where the generated power by this unit $P_{y,i,t}^{Y,H}$ is injected into the PDS at bus i . The same explanations also apply for the reactive power consumption of pumps and generation of small PSH in (7).

Connection of the pumps and PSH units to both power and water distribution systems is established through the mapping sets \mathcal{U}_i and \mathcal{Y}_i that map pump u and PSH unit y to the bus i in (6)-(7). By modeling the interdependence between power and water distribution systems, WDS electricity requirement and PSH generation can be represented as valuable sources of flexibility to the PDS operation. Integration of small PSH can provide additional flexibility and supply to the PDS operation, while optimizing the power consumption of pumps in the WDS, which indirectly improves PDS operation in terms of reducing peak-time energy requirements. Further details regarding WDS operation with the PSH unit are provided next.

3.3. Water Distribution System Constraints

The proposed model for the integration of small PSH in power and water distribution systems is subject to the operational constraints of the WDS, as well as the technical characteristics of pipes, pumps, tanks and small PSH unit in the WDS operation, formulated in (12)-(31). The PSH unit is modeled according to the characteristics described in Section 2, including the tank for water storage, the pump for charging tank, and the hydroelectric turbine for power generation from the discharging water flow.

3.3.1. Water Flow Constraint

The water flow constraint in the WDS is modeled in (12). According to this constraint, water flow from the reservoir nodes along with the input/output water flow from the tanks supply the WDS water requirement, where \mathbf{W}_t^R is $N \times 1$ vector of water inflows at the reservoir nodes at time t ; \mathbf{Q}_t is $J \times 1$ vector of volumetric flow in pipelines at time t ; \mathbf{A} is $N \times J$ node-arc incidence matrix; $\mathbf{C}_t/\mathbf{D}_t$ are the input/output water of tanks at

time t ; $\mathbf{\Lambda}^T$ is $T \times N$ tank-node matrix and \mathbf{W}_t^D is the water load of every node in the WDS at time t .

$$\mathbf{W}_t^R = \mathbf{A}\mathbf{Q}_t + \mathbf{\Lambda}^T (\mathbf{C}_t - \mathbf{D}_t) + \mathbf{W}_t^D, \quad \forall t. \quad (12)$$

3.3.2. Water Pumps Operation

The operation of water pumps in the WDS is proportional to the required pressure head rise and water flow. The pressure head rise in the WDS is modeled in (13), where \mathbf{B} is $U \times J$ pump-arc matrix; \mathbf{H}_t is $N \times 1$ vector of pressure head at water system nodes at time t ; $\mathbf{\Omega}_t$ is $U \times 1$ vector of pump speed at time t ; \odot and \oslash denote the component-wise matrix multiplication and division; a, b, c are specific pump parameters and $\mathbf{1}^U$ is $U \times 1$ vector of ones. The power consumption of pumps, expressed in (6)-(7), is modeled and bounded in (14)-(15), where η^P is the pump efficiency; \mathbf{P}_t^U is $U \times 1$ vector of power consumption of pumps at time t ; ρ is water density; g is acceleration due to gravity and $\underline{\mathbf{P}}^U, \overline{\mathbf{P}}^U$ are the lower and upper limits of pump power. Unidirectional pumping flow is enforced in (16), ensuring that water flows in one direction.

$$\mathbf{B}\mathbf{A}^T\mathbf{H}_t = \mathbf{\Omega}_t^2 \odot (a\mathbf{1}^U - (b(\mathbf{1}^U \oslash \mathbf{\Omega}_t) \odot \mathbf{B}\mathbf{Q}_t)^c), \quad \forall t, \quad (13)$$

$$\eta^P \mathbf{P}_t^U = \rho g (\mathbf{B}\mathbf{A}^T\mathbf{H}_t) \odot \mathbf{Q}_t, \quad \forall t, \quad (14)$$

$$\underline{\mathbf{P}}^U \leq \mathbf{P}_t^U \leq \overline{\mathbf{P}}^U, \quad \forall t, \quad (15)$$

$$\mathbf{B}\mathbf{Q}_t \geq 0, \quad \forall t. \quad (16)$$

3.3.3. Water Tank Operation

The water tank model, including the state equation of the tank, initial/target status of the tank, pressure head of the tank node, as well as charge and discharge constraints are presented in (17)-(23). Available water in the tank is expressed in (17)-(19), where \mathbf{V}_t is $T \times 1$ vector of available water in the tank at time t and $\mathbf{V}_{ini}, \mathbf{V}_{trg}$ are the initial and target volumes of water in the tank. The pressure head at the tank node is determined using the level of stored water in the tank in (20), where the $\mathbf{\Delta}$ is $T \times T$ diagonal matrix of tank surface value. The limits associated with the water volume and inputs/outputs (charge/discharge) of the tank are presented in (21)-(23), where $\underline{\mathbf{V}}, \overline{\mathbf{V}}$ are the lower and upper capacities of the tank; $\underline{\mathbf{C}},$

\underline{C} are the lower and upper limits of input water flow to the tank and \underline{D} , \overline{D} are lower and upper limits of released water flow from the tank.

$$\mathbf{V}_t = \mathbf{V}_{t-1} + \mathbf{C}_t - \mathbf{D}_t, \quad \forall t > 1, \quad (17)$$

$$\mathbf{V}_t = \mathbf{V}_{ini} + \mathbf{C}_t - \mathbf{D}_t, \quad \forall t = 1, \quad (18)$$

$$\mathbf{V}_t = \mathbf{V}_{trg}, \quad \forall t = 24, \quad (19)$$

$$\mathbf{V}_t = \Delta \mathbf{\Lambda} \mathbf{H}_t, \quad \forall t, \quad (20)$$

$$\underline{\mathbf{V}} \leq \mathbf{V}_t \leq \overline{\mathbf{V}}, \quad \forall t, \quad (21)$$

$$\underline{\mathbf{C}} \leq \mathbf{C}_t \leq \overline{\mathbf{C}}, \quad \forall t, \quad (22)$$

$$\underline{\mathbf{D}} \leq \mathbf{D}_t \leq \overline{\mathbf{D}}, \quad \forall t. \quad (23)$$

3.3.4. Pumped-Storage Hydropower Operation

The power consumption and generation of small PSH, reflected in (6), are modeled and bounded in (24)-(27), where $\mathbf{P}_t^{Y,P}$, $\mathbf{P}_t^{Y,H}$ are $Y \times 1$ vectors of consumed and generated power by the PSH units at time t ; η^H is turbine efficiency; $\mathbf{H}_t^{Y,P}$, $\mathbf{H}_t^{Y,H}$ are $Y \times 1$ vectors of head rise and available pressure head in pumping and generating modes of PSH units at time t ; $\mathbf{Q}_t^{Y,P}$, $\mathbf{Q}_t^{Y,H}$ are $Y \times 1$ vectors of the water flow charged/discharged to/from the PSH tank at time t ; $\underline{\mathbf{P}}^{Y,P}$, $\overline{\mathbf{P}}^{Y,P}$ are the lower and upper bounds of power consumption by PSH units and $\underline{\mathbf{P}}^{Y,H}$, $\overline{\mathbf{P}}^{Y,H}$ are the lower and upper bounds of power generation by PSH units.

$$\eta^P \mathbf{P}_t^{Y,P} = \rho g \mathbf{H}_t^{Y,P} \odot \mathbf{Q}_t^{Y,P}, \quad \forall t, \quad (24)$$

$$\mathbf{P}_t^{Y,H} = \eta^H \rho g \mathbf{H}_t^{Y,H} \odot \mathbf{Q}_t^{Y,H}, \quad \forall t, \quad (25)$$

$$\underline{\mathbf{P}}^{Y,P} \leq \mathbf{P}_t^{Y,P} \leq \overline{\mathbf{P}}^{Y,P}, \quad \forall t, \quad (26)$$

$$\underline{\mathbf{P}}^{Y,H} \leq \mathbf{P}_t^{Y,H} \leq \overline{\mathbf{P}}^{Y,H}, \quad \forall t. \quad (27)$$

3.3.5. Pressure Head Loss

The pressure head loss in the pipes is modeled according to the empirical Hazen-Williams pressure head loss model in (28), where \mathbf{G} is a $S \times S$ matrix of pipe resistance parameters and $\Pi(\cdot)$ is the unit sign function [24]. The limits of pressure head in each node and the volumetric flow in the pipes are presented in (29)-(30), where $\underline{\mathbf{H}}$, $\overline{\mathbf{H}}$ are the lower and upper limits of the pressure head in each node and $\underline{\mathbf{Q}}$, $\overline{\mathbf{Q}}$ are the lower and upper limits of volumetric water flow within the pipes. Finally, constraint (31) is enforced to fix the pressure head value in reservoir nodes, where Θ is $R \times N$ reservoir-node incidence matrix and \mathbf{Z} is $R \times 1$ vector of elevation at the reservoir nodes.

$$-\mathbf{A}^T \mathbf{H}_t = \mathbf{G} \Pi(\mathbf{Q}_t) |\mathbf{Q}_t|^{1.852}, \quad \forall t, \quad (28)$$

$$\underline{\mathbf{H}} \leq \mathbf{H}_t \leq \overline{\mathbf{H}}, \quad \forall t, \quad (29)$$

$$\underline{\mathbf{Q}} \leq \mathbf{Q}_t \leq \overline{\mathbf{Q}}, \quad \forall t, \quad (30)$$

$$\Theta \mathbf{H}_t = \mathbf{Z}, \quad \forall t. \quad (31)$$

3.4. Piecewise Linear Approximation

Considering the non-linear constraints within WDS operation in (13)-(14), (24)-(25) and (28), the proposed model for the integration of small PSH in power and water distribution systems is a mixed-integer non-linear programming (MINLP) problem, where the global optimum is not guaranteed. To address this issue, the mentioned non-linear constraints are approximated using the linear models described next.

3.4.1. Pressure Head Loss Function

Pressure head loss $L_{j,t}(Q_{j,t})$ in pipe j connecting two consecutive nodes is expressed as a function of water flow $Q_{j,t}$ in (32).

$$L_{j,t}(Q_{j,t}) = G_j \Pi(Q_{j,t}) |Q_{j,t}|^{1.852}, \quad \forall j, \forall t. \quad (32)$$

To approximate this function, we divide the $Q_{j,t}$ into $M - 1$ segments using the breakpoints $q_j^1, q_j^2, \dots, q_j^M$, where q_j^1 and q_j^M respectively coincide with the lower and upper limits of $Q_{j,t}$. Every m^{th} interval $[q_j^m, q_j^{m+1}]$ is linked to a binary variable $\beta_{j,t}^m$, and each breakpoint q_j^m is linked to a continuous variable $\alpha_{j,t}^m$, where $\alpha_{j,t}^m \in [0, 1]$. The water flow in WDS operation $Q_{j,t}$ can

be represented as a linear combination of consecutive breakpoints, weighted by the continuous variables in (33), as follows:

$$Q_{j,t} = \sum_{m=1}^M q_j^m \alpha_{j,t}^m, \quad \forall j, \forall t, \quad (33)$$

where $q_j^m \leq Q_{j,t} \leq q_j^{m+1}$. The linear approximation of pressure head loss function can be represented as a linear combination of function values evaluated at the breakpoints, weighted by continuous variables in (34). The number of active segments at each time t is limited to one in (35) and the number of consecutive positive continuous variables $\alpha_{j,t}^m$ that can take non-zero values is limited to two in (36)-(39).

$$\hat{L}_{j,t} = \sum_{m=1}^M L_{j,t}(q_j^m) \alpha_{j,t}^m, \quad \forall j, \forall t, \quad (34)$$

$$\sum_{m=1}^{M-1} \beta_{j,t}^m = 1, \quad \forall j, \forall t, \quad (35)$$

$$\sum_{m=1}^M \alpha_{j,t}^m = 1, \quad \forall j, \forall t, \quad (36)$$

$$\alpha_{j,t}^m \leq \beta_{j,t}^{m-1} + \beta_{j,t}^m, \quad -1, \forall j, \forall t, m = 2, \dots, M-1, \quad (37)$$

$$\alpha_{j,t}^1 \leq \beta_{j,t}^1, \quad \forall j, \forall t, \quad (38)$$

$$\alpha_{j,t}^M \leq \beta_{j,t}^{M-1}, \quad \forall j, \forall t. \quad (39)$$

3.4.2. Water Pump Constraints

The non-linear models for pressure head rise and power consumption of pump u are functions of pump speed $\Omega_{u,t}$ and water flow $Q_{u,t}$ in (40)-(41).

$$\Delta H_{u,t}(\Omega_{u,t}, Q_{u,t}) = \Omega_{t,u}^2 (a - b(\frac{1}{\Omega_{u,t}})^c), \quad \forall u, \forall t, \quad (40)$$

$$P_{u,t}^U(\Omega_{u,t}, Q_{u,t}) = \rho g \Omega_{t,u}^2 (a - b(\frac{1}{\Omega_{u,t}} Q_{u,t})^c) Q_{u,t} / \eta^P, \quad \forall u, \forall t. \quad (41)$$

To approximate these functions, we divide $Q_{u,t}$ into $K-1$ segments using the breakpoints $q_u^1, q_u^2, \dots, q_u^K$, where q_u^1 and q_u^K respectively coincide with the

lower and upper limits of $Q_{u,t}$. Similarly, we divide $\Omega_{t,u}$ into $E-1$ segments using the breakpoints $\omega_u^1, \omega_u^2, \dots, \omega_u^E$, where ω_u^1 and ω_u^E respectively coincide with the lower and upper limits of $\Omega_{u,t}$. The segments on the axes partition the function domain into several rectangles. Consider the rectangle defined by the vertices (q_u^k, ω_u^e) , (q_u^{k+1}, ω_u^e) , $(q_u^{k+1}, \omega_u^{e+1})$ and (q_u^k, ω_u^{e+1}) on the function domain, which is divided into two separate triangles using the diagonal (q_u^k, ω_u^e) and $(q_u^{k+1}, \omega_u^{e+1})$. The upper left and lower right triangles are respectively linked to the binary variables $\bar{h}_{u,t}^{k,e}$ ($k=1, 2, \dots, K-1$ and $e=2, \dots, E$), and $\underline{h}_{u,t}^{k,e}$ ($k=2, \dots, K$ and $e=1, 2, \dots, E-1$). Also, each vertex (k, e) is linked to a continuous variable $\alpha_{u,t}^{k,e}$, where $\alpha_{u,t}^{k,e} \in [0, 1]$. Water flow rate and speed for pump u at time t are represented as linear combinations of the vertex coordinates weighted by the respective continuous variables $\alpha_{u,t}^{k,e}$ in (42)-(43).

$$Q_{u,t} = \sum_{k=1}^K \sum_{e=1}^E q_u^k \alpha_{u,t}^{k,e}, \quad \forall u, \forall t, \quad (42)$$

$$\Omega_{u,t} = \sum_{k=1}^K \sum_{e=1}^E \omega_u^e \alpha_{u,t}^{k,e}, \quad \forall u, \forall t, \quad (43)$$

where $q_u^k \leq Q_{t,u} \leq q_u^{k+1}$ and $\omega_u^e \leq \Omega_{t,u} \leq \omega_u^{e+1}$. The linear functions to model the pressure head rise and power consumption of pump u at time t are expressed as combination of the function values evaluated at the break-points, weighted by the continuous variables $\alpha_{u,t}^{k,e}$ in (44)-(45). The number of activated triangles in any solution is constrained to be one in (46) and the number of consecutive positive continuous variables $\alpha_{u,t}^{k,e}$ that can take non-zero values is limited to three in (47)-(48).

$$\Delta \hat{H}_{u,t} = \sum_{k=1}^K \sum_{e=1}^E \Delta H_{u,t}(q_u^k, \omega_u^e) \alpha_{u,t}^{k,e}, \quad \forall u, \forall t, \quad (44)$$

$$\hat{P}_{u,t}^U = \sum_{k=1}^K \sum_{e=1}^E P_{u,t}^U(q_u^k, \omega_u^e) \alpha_{u,t}^{k,e}, \quad \forall u, \forall t, \quad (45)$$

$$\sum_{k=1}^K \sum_{e=1}^E (\bar{h}_{u,t}^{k,e} + \underline{h}_{u,t}^{k,e}) = 1, \quad \forall u, \forall t, \quad (46)$$

$$\sum_{k=1}^K \sum_{e=1}^E \alpha_{u,t}^{k,e} = 1, \quad \forall u, \forall t, \quad (47)$$

$$\alpha_{u,t}^{k,e} \leq \bar{h}_{u,t}^{k,e-1} + \bar{h}_{u,t}^{k+1,e} + \bar{h}_{u,t}^{k,e} + \underline{h}_{u,t}^{k-1,e} + \underline{h}_{u,t}^{k,e+1} + \underline{h}_{u,t}^{k,e}, \quad \forall k, \forall e, \forall u, \forall t. \quad (48)$$

3.4.3. Pumped-Storage Hydropower Constraints

Power consumption and generation of the small PSH y are expressed as functions of pressure head and charging/discharging water flows in (49)-(50).

$$P_{y,t}^{Y,P}(\Delta H_{y,t}^{Y,P}, Q_{y,t}^{Y,P}) = \rho g \Delta H_{y,t}^{Y,P} Q_{y,t}^{Y,P} / \eta^P, \quad \forall y, \forall t, \quad (49)$$

$$P_{y,t}^{Y,H}(\Delta H_{y,t}^{Y,H}, Q_{y,t}^{Y,H}) = \rho g \Delta H_{y,t}^{Y,H} Q_{y,t}^{Y,H} \eta^H, \quad \forall y, \forall t. \quad (50)$$

In order to approximate the non-linear power consumption function in (49), we divide $Q_{y,t}^{Y,P}$ into $\Phi - 1$ segments using the breakpoints $q_y^1, q_y^2, \dots, q_y^\Phi$, where q_y^1 and q_y^Φ respectively coincide with the lower and upper limits of $Q_{y,t}^{Y,P}$. We also divide $\Delta H_{y,t}^{Y,P}$ into $\Psi - 1$ segments using the breakpoints $\chi_y^1, \chi_y^2, \dots, \chi_y^\Psi$, where χ_y^1 and χ_y^Ψ respectively coincide with the lower and upper limits of $\Delta H_{y,t}^{Y,P}$. Assume the rectangle defined by the vertices (q_y^ϕ, χ_y^ψ) , $(q_y^{\phi+1}, \chi_y^\psi)$, $(q_y^{\phi+1}, \chi_y^{\psi+1})$ and $(q_y^\phi, \chi_y^{\psi+1})$ on the function domain. The rectangle with the specified vertices is divided into two separate triangles using the diagonal (q_y^ϕ, χ_y^ψ) and $(q_y^{\phi+1}, \chi_y^{\psi+1})$. The upper left and lower right triangles are respectively linked to the binary variables $\overline{\Delta h}_{y,t}^{\phi,\psi}$ ($\phi = 1, 2, \dots, \Phi - 1$ and $\psi = 2, \dots, \Psi$), and $\underline{\Delta h}_{y,t}^{\phi,\psi}$ ($\phi = 2, \dots, \Phi$ and $\psi = 1, 2, \dots, \Psi - 1$). Also, each vertex (ϕ, ψ) is linked to a continuous variable $\delta_{y,t}^{\phi,\psi}$, where $\delta_{y,t}^{\phi,\psi} \in [0, 1]$. Water flow rate $Q_{y,t}^{Y,P}$ and pressure head rise $\Delta H_{y,t}^{Y,P}$ for PSH y at time t are represented as linear combinations of the vertices' coordinates weighted by the continuous variables $\delta_{y,t}^{\phi,\psi}$ in (51)-(52).

$$Q_{y,t}^{Y,P} = \sum_{\phi=1}^{\Phi} \sum_{\psi=1}^{\Psi} q_y^\phi \delta_{y,t}^{\phi,\psi}, \quad \forall y, \forall t, \quad (51)$$

$$\Delta H_{y,t}^{Y,P} = \sum_{\phi=1}^{\Phi} \sum_{\psi=1}^{\Psi} \chi_y^\psi \delta_{y,t}^{\phi,\psi}, \quad \forall y, \forall t, \quad (52)$$

where $q_y^\phi \leq Q_{y,t}^{Y,P} \leq q_y^{\phi+1}$ and $\chi_y^\psi \leq \Delta H_{y,t}^{Y,P} \leq \chi_y^{\psi+1}$. The linear function to model power consumption of PSH y at time t is expressed as combination of the function values evaluated at the breakpoints, weighted by the continuous variables $\delta_{y,t}^{\phi,\psi}$ in (53). The number of activated triangles in any solution is limited to one in (54) and the number of consecutive positive continuous variables taking non-zero values is limited to three in (55)-(56).

$$\hat{P}_{y,t}^{Y,P} = \sum_{\phi=1}^{\Phi} \sum_{\psi=1}^{\Psi} P_{y,t}^{Y,P}(\chi_y^\psi, q_y^\phi) \delta_{y,t}^{\phi,\psi}, \quad \forall y, \forall t, \quad (53)$$

$$\sum_{\phi=1}^{\Phi} \sum_{\psi=1}^{\Psi} (\overline{\Delta h}_{y,t}^{\phi,\psi} + \underline{\Delta h}_{y,t}^{\phi,\psi}) = 1, \quad \forall y, \forall t, \quad (54)$$

$$\sum_{\phi=1}^{\Phi} \sum_{\psi=1}^{\Psi} \delta_{y,t}^{\phi,\psi} = 1, \quad \forall y, \forall t, \quad (55)$$

$$\begin{aligned} \delta_{y,t}^{\phi,\psi} \leq & \overline{\Delta h}_{y,t}^{\phi,\psi-1} + \overline{\Delta h}_{y,t}^{\phi+1,\psi} + \overline{\Delta h}_{y,t}^{\phi,\psi} \\ & + \underline{\Delta h}_{y,t}^{\phi-1,\psi} + \underline{\Delta h}_{y,t}^{\phi,\psi+1} + \underline{\Delta h}_{y,t}^{\phi,\psi}, \quad \forall \phi, \forall \psi, \forall y, \forall t. \end{aligned} \quad (56)$$

In order to approximate the non-linear power generation model of the PSH unit in (50), we first divide $Q_{y,t}^{Y,H}$ and $\Delta H_{y,t}^{Y,H}$ into $\Upsilon-1$ and $\Pi-1$ segments using the breakpoints $q_y^1, q_y^2, \dots, q_y^\Upsilon$ and $\chi_y^1, \chi_y^2, \dots, \chi_y^\Pi$, where q_y^1, q_y^Υ respectively coincide with the lower and upper limits of $Q_{y,t}^{Y,H}$; and χ_y^1, χ_y^Π respectively coincide with the lower and upper limits of $\Delta H_{y,t}^{Y,H}$. Consider the rectangle shaped by the vertices (q_y^v, χ_y^π) , (q_y^{v+1}, χ_y^π) , $(q_y^{v+1}, \chi_y^{\pi+1})$ and $(q_y^v, \chi_y^{\pi+1})$ on the function domain, which is divided into two separate triangles using the diagonal (q_y^v, χ_y^π) and $(q_y^{v+1}, \chi_y^{\pi+1})$. The upper left and lower right triangles are respectively linked to the binary variables $\overline{\Delta h}_{y,t}^{v,\pi}$ ($v=1, 2, \dots, \Upsilon-1$ and $\pi=2, \dots, \Pi$), and $\underline{\Delta h}_{y,t}^{v,\pi}$ ($v=2, \dots, \Upsilon$ and $\pi=1, 2, \dots, \Pi-1$). Each vertex (v, π) is linked to a continuous variable $\delta_{y,t}^{v,\pi}$, where $\delta_{y,t}^{v,\pi} \in [0, 1]$. Water flow rate $Q_{y,t}^{Y,H}$ and available head $\Delta H_{y,t}^{Y,H}$ for PSH y at time t are represented as linear combinations of the vertices' coordinates weighted by the respective continuous variables $\delta_{y,t}^{v,\pi}$ in (57)-(58).

$$Q_{y,t}^{Y,H} = \sum_{v=1}^{\Upsilon} \sum_{\pi=1}^{\Pi} q_y^v \delta_{y,t}^{v,\pi}, \quad \forall y, \forall t, \quad (57)$$

$$\Delta H_{y,t}^{Y,H} = \sum_{v=1}^{\Upsilon} \sum_{\pi=1}^{\Pi} \chi_y^\pi \delta_{y,t}^{v,\pi}, \quad \forall y, \forall t, \quad (58)$$

where $q_y^v \leq Q_{y,t}^{Y,H} \leq q_y^{v+1}$ and $\chi_y^\pi \leq \Delta H_{y,t}^{Y,H} \leq \chi_y^{\pi+1}$. The linear function to model power generation of PSH is expressed as combination of the function

values evaluated at the breakpoints, weighted by the continuous variables $\delta_{y,t}^{v,\pi}$ in (59). The number of activated triangles in any solution is limited to one in (60) and the number of consecutive positive continuous variables that take non-zero values is limited to three in (61)-(62).

$$\hat{P}_{y,t}^{Y,H} = \sum_{v=1}^{\Upsilon} \sum_{\pi=1}^{\Pi} P_{y,t}^{Y,H}(\chi_y^\pi, q_y^v) \delta_{y,t}^{v,\pi}, \quad \forall y, \forall t, \quad (59)$$

$$\sum_{v=1}^{\Upsilon} \sum_{\pi=1}^{\Pi} (\overline{\Delta h}_{y,t}^{v,\pi} + \underline{\Delta h}_{y,t}^{v,\pi}) = 1, \quad \forall y, \forall t, \quad (60)$$

$$\sum_{v=1}^{\Upsilon} \sum_{\pi=1}^{\Pi} \delta_{y,t}^{v,\pi} = 1, \quad \forall y, \forall t, \quad (61)$$

$$\delta_{y,t}^{v,\pi} \leq \overline{\Delta h}_{y,t}^{v,\pi-1} + \overline{\Delta h}_{y,t}^{v+1,\pi} + \overline{\Delta h}_{y,t}^{v,\pi} + \underline{\Delta h}_{y,t}^{v-1,\pi} + \underline{\Delta h}_{y,t}^{v,\pi+1} + \underline{\Delta h}_{y,t}^{v,\pi}, \quad \forall y, \forall t. \quad (62)$$

Applying the approximation models in (32)-(62), the ultimate model for integrating small PSH in power and water distribution systems operation is formulated as a MISOCP problem, solvable using commercial solvers, e.g., CPLEX. Further details regarding the implementation of approximation models in (32)-(62) can be found in [4, 25].

4. Numerical Results

The proposed model for the integration of small PSH unit in power and water distribution systems is implemented on a 33-bus test PDS and a 16-node test WDS, which are depicted in Fig. 4. The water test system integrated with the small PSH unit includes one water reservoir (node 1), two water tanks (nodes 14 and 16), three water pumps (pipes 1, 4 and 15), and one hydropower generator (pipe 16). The power generated by the hydropower unit is injected into the PDS through bus 2, and the power for the operation of pumps is extracted from buses 2, 12 and 24. The operating efficiency of pumps and PSH unit turbine are assumed to be 85% and 90%, respectively, and the power factor associated with the operation of pumps and PSH is assumed to be 0.8. The initial and target water volumes for both WDS and PSH tanks are 1200 m³ and the PDS feed-in tariff for discharge power of small PSH is assumed to be 0.03\$/kWh. The hourly upstream grid price and electricity load data of California Independent System Operator (CAISO) for

March 29-30, 2017, depicted in Fig. 5, are used for the simulations [26]. The hourly water demand profile in the WDS along with the time-of-use (TOU) and dynamic electricity tariffs is shown in Fig. 6. The scheduling horizon in the studied problem, NT , is set to be 24. Rest of the data for the IEEE 33-bus test system and 16-node water system can be found in [27]. In order to accommodate the power demand of 16-node WDS in the 33-bus test power system, the active and reactive power loads in the PDS are scaled down to 70% of the original system rated active and reactive loads of 3,715 kW and 2,300 kVAr.

Four cases are studied to evaluate the impact of the PSH unit, its flexibility, and the proposed coordinated operation model in the operation cost of PDS:

- In Case 1, WDS operation is optimized independently and not coordinated with the PDS optimization, with its power consumption defined by fixed power profiles. In addition, no PSH power generation is considered.
- In Case 2, the effect of integrating small PSH is evaluated by adding its power generation as a fixed profile to Case 1. This generation profile is obtained from independent optimization of WDS operation with PSH.
- In Case 3, the PDS operation is optimized with the coordinated operation of the WDS considering both power and water distribution systems operational constraints. In this case, no PSH power generation is considered.
- In Case 4, the PDS operation is coordinated with the operation of WDS connected to the small PSH system. The flexibility introduced by the charge and discharge of PSH unit in this case enables the PDS operator to further coordinate the operation of PDS with the WDS operation and manage the energy demand in the PDS, while benefiting from distributed hydropower generation.

The proposed model for the coordinated operation of power and water distribution systems with the small PSH unit is modeled as a MISOCP problem and solved using CPLEX solver on a desktop computer with a 4.0-GHz i7 processor and 32 GB of RAM. The computation time for solving the proposed model in study Cases 1-4 is respectively 0.817, 0.889, 2.546, and 9.946 seconds.

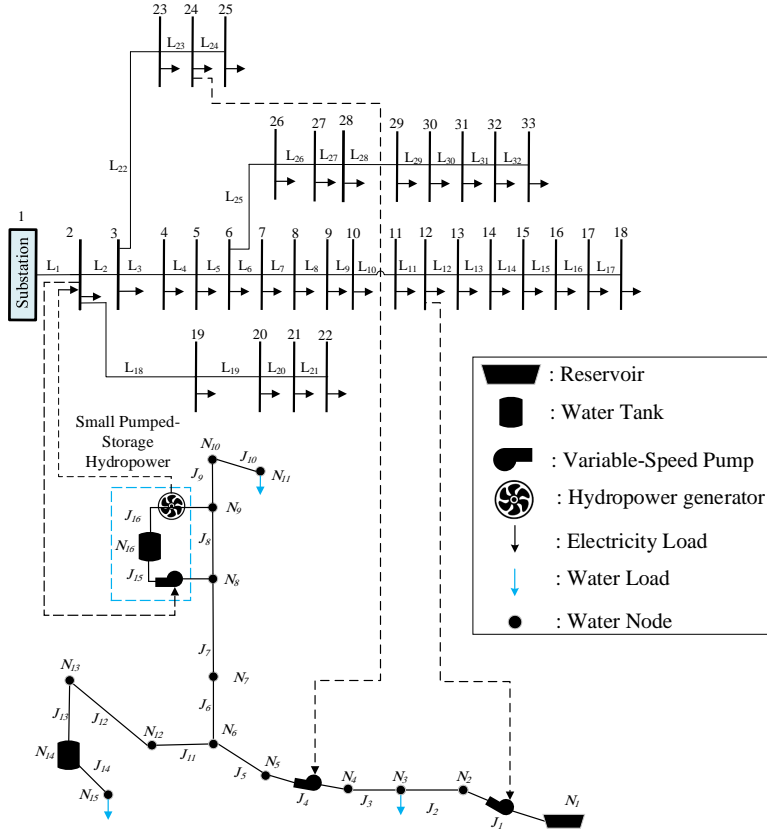


Figure 4: IEEE 33-bus test power distribution system connected to the 16-node test water distribution system.

4.1. Operation Cost of Power Distribution System

The operation cost of 33-bus PDS in the four study cases is summarized in Table 1 and analyzed for each case next.

Table 1: Operation Cost of 33-bus Power Distribution System

Study Case	Case 1	Case 2	Case 3	Case 4
Operation cost (\$)	2,542	2,494.4	2,523.5	2,413.5
Cost reduction compared to Case 1 (%)	–	1.87	0.72	5.05

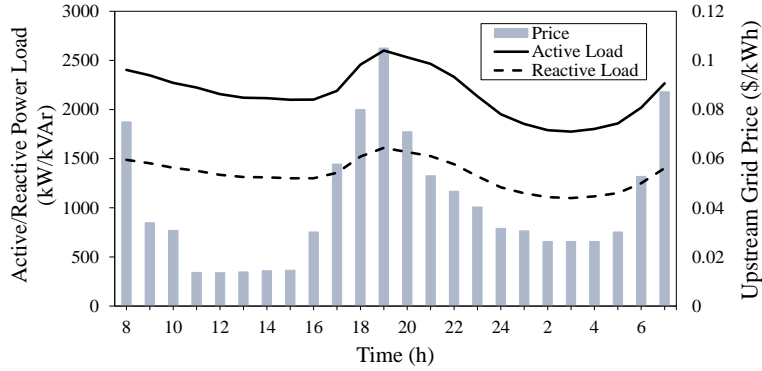


Figure 5: Active/reactive load and upstream grid price.

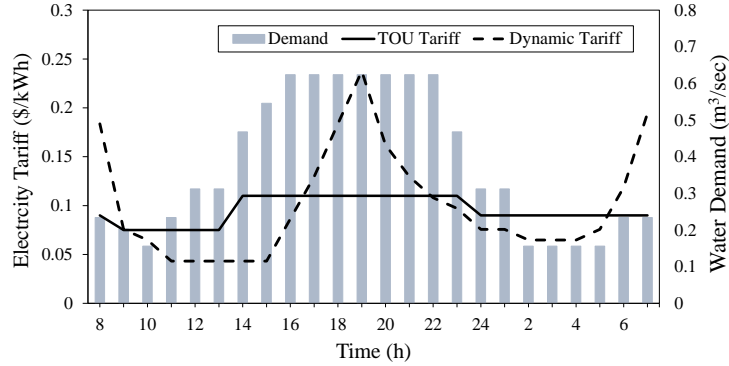


Figure 6: Water demand and electricity tariff.

4.1.1. Case 1: PDS Operation with Uncoordinated Operation of WDS

In this case, the PDS operator optimizes the system operation considering a forecast of power consumption in the WDS, provided by the operator of this system. This implies that the operator of PDS has no control over the power consumption of water system and its available flexibility. The operation cost of PDS in this case is \$2,542 that accounts for the cost of power purchased from the upstream grid. As the WDS operation is not coordinated with the PDS operation and no PSH is integrated to deliver flexibility, the PDS operator cannot further optimize the system performance in this case.

4.1.2. Case 2: PDS Operation with Uncoordinated Operation of WDS and PSH

In this case, the uncoordinated operation of small PSH unit is added into the studied problem in Case 1, where uncoordinated charge and discharge rates are applied to model the PSH benefit for the PDS operation. These rates are obtained through separate operation of the WDS with small PSH based on the electricity tariff. According to the numerical results, the operation cost of PDS in this case is \$2,494.4, which is associated with the costs of power purchased from the upstream grid and small PSH. Compared to Case 1, the operation cost in Case 2 is reduced by 1.87%. Such a cost reduction is mainly due to the energy flexibility that small PSH provides and by enabling load shifting, it leads to peak load shaving and cost-efficient operation of the PDS.

4.1.3. Case 3: PDS with Coordinated Operation of WDS

In this case, the operation of PDS is optimized with the coordinated operation of WDS with no PSH unit being integrated into the operation of these systems. The decisions upon purchasing power from the upstream grid are affected by WDS operation since water demand must be supplied with respect to all hydraulic constraints. By considering the time-varying water demand in the WDS and electricity prices in the upstream grid, PDS operation is optimized with the appropriate functioning of pumps in WDS. According to the simulation results, the daily operation cost of the PDS is \$2,523.5, which represents a reduction of 0.72% compared to Case 1. This reduction is perceived from the flexible power consumption of water pumps in the water system that enables the PDS operator to shift the power requirement of WDS in accordance with electricity prices in the upstream grid.

4.1.4. Case 4: PDS with Coordinated Operation of WDS and PSH

In this case, the PDS operation is optimized with the coordinated operation of small PSH unit, integrated into the WDS operation. Considering the electricity prices in the upstream grid and also feed-in tariff in the PDS, system operator controls the charging and discharging processes of small PSH unit to get benefit from the energy flexibility, while serving the PDS demand and pumping power requirements in the water system. The obtained flexibility leads to cost-efficient power procurement from the upstream grid with respect to the prices, since the operation cost of PDS reduces to \$2,413.5.

Compared to Cases 1, 2 and 3, the operation cost in Case 4 is respectively reduced by 5.05%, 3.24%, and 4.35%, indicating the considerable role of small PSH and its coordinated operation in the reduction of PDS operation cost. The small PSH unit takes advantage of both power and water systems to serve as an energy storage device, providing energy flexibility that is reflected in the operation of power and water distribution systems. While discharging water into the WDS, water demand is partially supplied from the water stored during the lower electricity price hours, reducing the pumping requirements to convey water from the reservoir to the demand. This effect is extended to the PDS operation, reducing the power purchased from the upstream grid at peak hours and minimizing the total operation cost. The optimal charge/discharge of the small PSH unit helps the PDS operator to manage the energy demand in the PDS, while controlling the operation of water pumps in the WDS. The detailed discussions associated with these results and the PSH effect on power and water distribution systems operation are presented in the following subsection.

4.2. PSH Flexibility Analysis

The comparison of power procured from the upstream grid in the study cases is presented in Fig. 7. In Fig. 7, when the PDS operation is optimized with the uncoordinated operation of WDS and no PSH integration, the peak consumption matches with the highest electricity price time step, and the PDS operator supplies the peak power demand with higher prices as there is no flexibility to control the power consumption and then power procurement from the upstream grid.

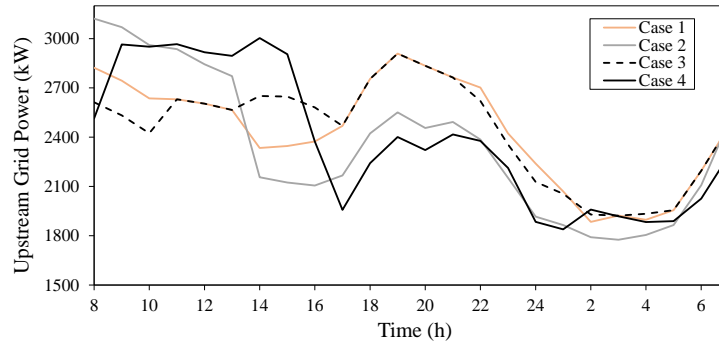


Figure 7: Purchased power from the upstream grid.

In Case 2, the power purchased from the upstream grid is significantly increased in off-peak hours, which is associated with the power requirements of the small PSH units for pumping and water storage. During peak hours, the small PSH discharges water and power to support the PDS and reduce the power requirement of pumps in the WDS, which consequently shifts the power system peak power consumption and offers an opportunity for its operator to reduce the cost of power procurement from the upstream grid.

In Case 3, power procurement from the upstream grid is slightly shifted from mid-peak hours to off-peak hours, where the electricity price is lower, compared to Case 1. In Fig. 7, the power procured from upstream grid in Case 3 is increased during the cheaper electricity price hours, 13:00-16:00, to energize water pumps in the WDS with the lowest possible cost, while meeting the hydraulic constraints in the WDS. In Case 4, PDS operation is optimized considering the flexibility gained from the pumping power consumption and power generation from the PSH. As the PDS operation is optimized with the coordinated operation of water system that is equipped with small PSH, improved results are expected, compared to the previous cases. According to results in this case, the PDS operator supplies more power to energize pumps in the water system and charge the small PSH during the first hours of the study period, 9:00-15:00, where electricity prices are lower. Later, in peak hours, 17:00-02:00, it benefits from discharge power of small PSH to supply PDS electricity requirement and meanwhile utilizes the discharge water to partially supply water demand in the WDS, which reduces the water requirement from the reservoir node and the power required for pumps' operation. This is evident in Fig. 8, where by integrating PSH unit into coordinated operation of power and water distribution systems, the water flow from reservoir to supply the load in the water node 11 during peak-time hours is almost zero.

The results in Figs. 7-8 for Cases 2 and 4 are proportional to PSH charging and discharging processes, shown in Fig. 9, where the positive values indicate power consumption during the pumping (charging) process, while the negative ones indicate power generation during the tank discharge. In Fig. 9, the small PSH operation in the model prioritizes the power purchase at initial hours based on the upstream grid price, different from the uncoordinated operation in Case 2, where the power consumption optimization relies on the electricity tariff. As shown, with pumping more water during the off-peak hours and storing it within the PSH tank, the discharged power by this unit during peak hours increases. The increase of discharged power, whose

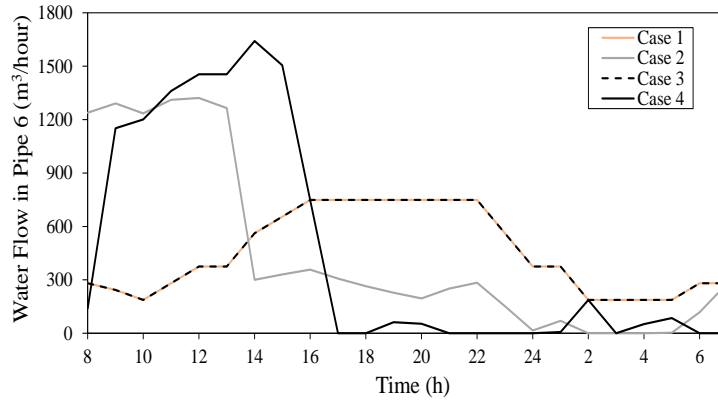


Figure 8: Water flow of pipe 6 in water distribution system.

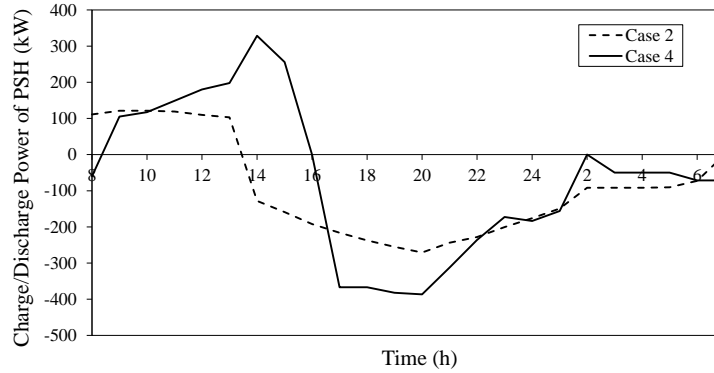


Figure 9: Charge/discharge power of pumped-storage hydropower.

injection into PDS would be cost-efficient, is achieved by an increased discharge flow rate of water that consequently leads to the least possible power consumption of pumps in the WDS to pump the water, as the discharged water by PSH provides support to supply the water demand and reduces the water requirement from the reservoir node (see Fig. 8).

The charge/discharge of small PSH unit is directly related to the tank flow rate and water level in tanks, as shown in Figs. 10-11. In Figs. 10-11, to store water during the off-peak hours, the PSH pump is energized and water is pumped into the tank, increasing the level of water available in the tank. When the water discharge is required for power generation, the tank is discharged and while supplying the water demand, the adequate condition for the WDS operation is ensured in terms of the pressure head.

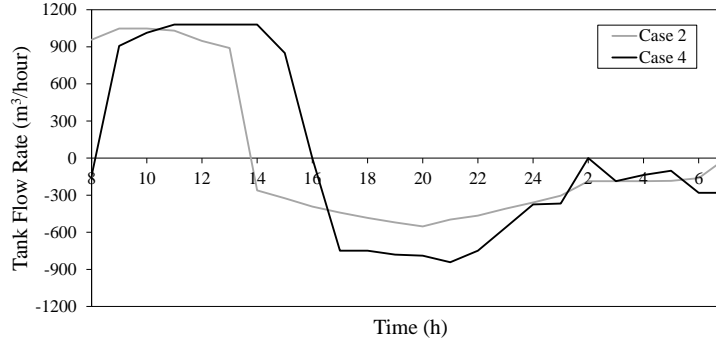


Figure 10: Water flow rate of pumped-storage hydropower tank.

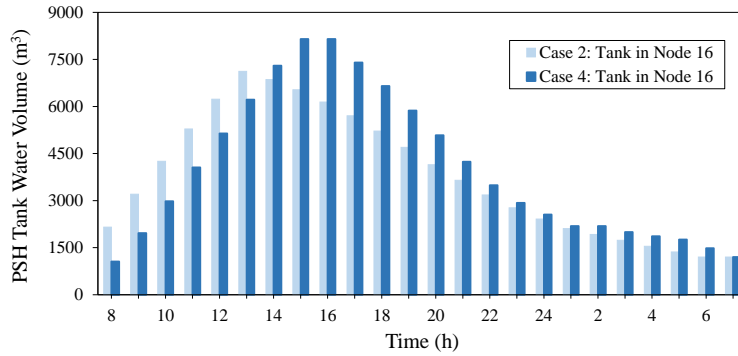


Figure 11: Available water in pumped-storage hydropower tank.

By coordinating the operation between the two systems, the operational variables of each system, represented by the voltages in the PDS and pressure head in the WDS, are in safe intervals, especially at hours of higher energy consumption. The voltage profile for Cases 1 and 4 at the highest demand period is shown in Fig. 12. As shown, by introducing PSH flexibility into the operation of the PDS in Case 4, the voltage profile along the grid is improved. On the other side, the changes on the pressure head level caused by the integration of small-scale PSH in WDS operation are bounded to the maximum pressure head level, as shown in Fig. 13.

4.3. Operation Cost of Water Distribution System

The results demonstrated that the integration of small PSH in coordinated operation of power and water distribution systems helps the PDS operator to efficiently utilize WDS flexibility in managing peak electricity

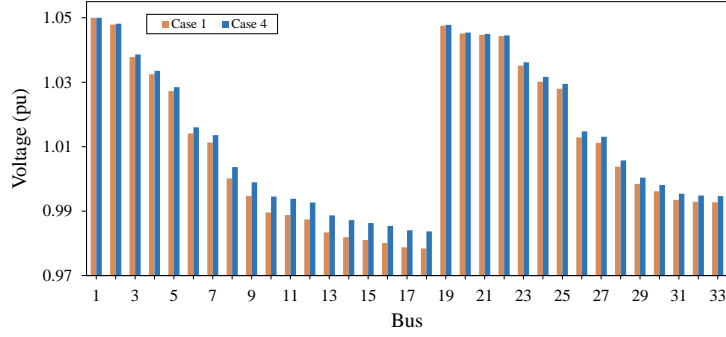


Figure 12: Voltage profile along the power grid.

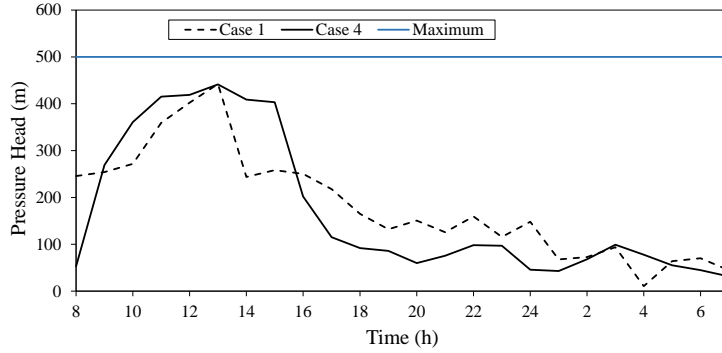


Figure 13: Pressure head at the reservoir node.

requirements, thereby reducing the operation cost of PDS. More specifically, the results showed that the PSH unit can supply local generation to PDS operation, while leveraging the flexible operation of water tanks and pumps to optimize electricity consumption in the WDS, which is reflected in the rate of transacted power from transmission system by the PDS operator. However, applying the proposed coordination scheme to capture WDS flexibility in favor of PDS operation may enforce additional expenses to WDS operation in terms of increasing power and water consumption rates.

To avoid any additional expenses in the coordinated operation of WDS in Cases 3 and 4, different from the the TOU tariff applied to uncoordinated WDS operation in Cases 1 and 2, the PDS operator applies dynamic tariff to charge the electricity consumption of WDS in a much more flexible manner. By implementing the dynamic electricity tariff, any additional expenses enforced to WDS operation due to the increase in water and power usages can

be compensated, as reflected in Table 2. The results in Table 2 clearly show that implementing the dynamic electricity tariff scheme along with adding PSH unit and its flexibility to the coordinated operation of power and water distribution systems ensures cost-efficient operation of both systems in supplying power and water demands, without violating power and water flow limits.

Table 2: Total Operation Cost of Power and Water Distribution Systems

Study Case	Case 1	Case 2	Case 3	Case 4
PDS operation cost (\$)	2,542	2,494.4	2,523.5	2,413.5
WDS operation cost (\$)	631.5	572.3	613.2	512.7
Total operation cost (\$)	3,173.5	3,066.7	3,136.7	2,926.2
Total cost reduction compared to Case 1 (%)	–	3.36	1.15	7.79

4.4. PSH Flexibility Analysis in a 123-bus Power Distribution System

In this section, the performance of the proposed model is assessed on a 123-bus test PDS [28] connected to the 16-node test WDS. The water pumps and PSH located at pipes 1, 4 and 15 in the WDS are connected to the PDS through buses 48, 77 and 7, respectively. The power generated from the PSH discharge is injected into the PDS at bus 7. To accommodate the WDS energy consumption, the active and reactive demand in [28] are scaled down to the 70% of the rated active and reactive power loads of 4,100 kW and 1,880 kVAr. The simulations are conducted based on the price data described in the first part of this section.

The operation of the interconnected IEEE 123-bus PDS and 16-node is evaluated with and without the proposed coordinated approach. Total operation cost of the PDS in the uncoordinated and coordinated cases is respectively \$2,277.80 and \$2,212.90, indicating the performance of the proposed model to reduce the operation cost of the PDS by 2.84%. The power consumed by the water pumps in the WDS, as well as the generated power by the hydropower unit in the coordinated case is shown in Fig. 14. In Fig. 14, the power consumption of pumps scheduled by the proposed coordination model follows the upstream grid prices. More specifically, the water pumps and PSH are energized in off-peak hours to pump water and ensure sufficient storage of water in the tanks. Later, the stored water is released to supply the water load in the WDS and generate electricity, which is consistent with the economic results obtained for the IEEE 33-bus test system.

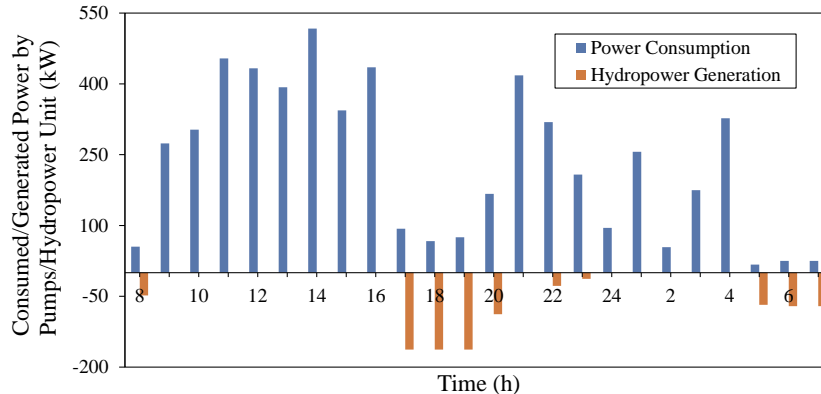


Figure 14: Consumed/Generated power by water pumps/hydropower unit.

The number of decision variables and the simulation time for implementing the proposed day-ahead coordination model on the IEEE 33-bus and 123-bus test PDS connected to the 16-node test WDS are summarized in Table 3. In Table 3, the number of decision variables and consequently the solution time are larger for the 123-bus system, though the solution time is considered very fast for the proposed model that is solved in day-ahead operation.

Table 3: Number of decision variables and simulation time for two test systems in Case 4.

Test power and water distribution systems	Number of decision variables	Simulation time (second)
33-bus PDS & 16-node WDS	16,297	9.946
123-bus PDS & 16-node WDS	28,345	39.28

5. Conclusion

PSH is a promising energy storage technology to improve the flexibility of power system. PSH requires water infrastructure, which can either be standalone or integrated with the existing infrastructure. This paper presented an optimization model for coordinating the operation of small PSH units with power and water distribution systems. The proposed model deploys different electricity tariff schemes and coordinates PSH operation in both pumping and generating modes with the operation of power and water distribution systems from economic perspectives. The proposed model is

implemented on the 33-bus and 123-bus test PDSs and a 16-node test WDS that are interdependent through a PSH unit and multiple pumping stations. Multiple cases are designed and studied to capture various impacts of PSH integration on the interdependent operation of power and water distribution systems. According to the simulation results, integrating small PSH unit into the operation of power and water distribution systems, in both uncoordinated and coordinated modes, leads to improved performance of PDS. The results showed that positive impacts of PSH become more significant in the coordinated operation of power and water systems, where the generated power by PSH unit supplies the power demand in the PDS and the flexibility provided by this unit leads to the reduction of required power by WDS for pumping water in peak hours, thus reducing the cost of supplying energy demand in the PDS. On the other side, implementing the dynamic tariff by PDS operator in the coordinated operation of power and water distribution systems with small PSH unit reduces the cost of energy consumption in the WDS. These results exhibit the potential of PSH to increase the economic efficiency of interdependent power and water distribution systems, while supplying local power and water to the operation of both systems. Future works include developing a model for coordinated operation of power and water systems in real-time operation, taking into account the delay in the water flow from the reservoir node to the load points in the WDS. Developing models for optimal sizing PSH components to deliver the most benefit to power and water distribution systems operation is also in order.

References

- [1] P. O’connor, B. Saulsbury, B. Hadjerioua, B. T. Smith, M. Bevelhimer, B. M. Pracheil, S.-C. Kao, R. A. Mcmanamay, N. M. Samu, R. Uria Martinez, et al., Hydropower vision a new chapter for america’s 1st renewable electricity source, Tech. rep., Oak Ridge National Lab.(ORNL), Oak Ridge, TN (United States) (2016).
- [2] K. Oikonomou, M. Parvania, Deploying water treatment energy flexibility in power distribution systems operation, in: 2020 IEEE Power & Energy Society Innovative Smart Grid Technologies Conference (ISGT), IEEE, 2020, pp. 1–5.
- [3] K. Oikonomou, M. Parvania, Optimal coordinated operation of interde-

- pendent power and water distribution systems, *IEEE Transactions on Smart Grid* 11 (6) (2020) 4784–4794.
- [4] K. Oikonomou, M. Parvania, Optimal coordination of water distribution energy flexibility with power systems operation, *IEEE Transactions on Smart Grid* 10 (1) (2018) 1101–1110.
 - [5] Q. Li, S. Yu, A. S. Al-Sumaiti, K. Turitsyn, Micro water–energy nexus: Optimal demand-side management and quasi-convex hull relaxation, *IEEE Transactions on Control of Network Systems* 6 (4) (2018) 1313–1322.
 - [6] K. Oikonomou, M. Parvania, Optimal participation of water desalination plants in electricity demand response and regulation markets, *IEEE Systems Journal* (2019).
 - [7] M. A. Sari, M. Badruzzaman, C. Cherchi, M. Swindle, N. Ajami, J. G. Jacangelo, Recent innovations and trends in in-conduit hydropower technologies and their applications in water distribution systems, *Journal of environmental management* 228 (2018) 416–428.
 - [8] M. Majidi, L. Rodriguez-Garcia, M. Parvania, T. M. Mosier, Integration of small pumped storage hydropower units in water distribution system operation, in: *2020 IEEE Power & Energy Society General Meeting (PESGM)*, IEEE, 2020, pp. 1–5.
 - [9] S. Rehman, L. M. Al-Hadhrami, M. M. Alam, Pumped hydro energy storage system: A technological review, *Renewable and Sustainable Energy Reviews* 44 (2015) 586–598.
 - [10] M. Petrollese, P. Seche, D. Cocco, Analysis and optimization of solar-pumped hydro storage systems integrated in water supply networks, *Energy* 189 (2019) 116176.
 - [11] A. Stoppato, A. Benato, N. Destro, A. Mirandola, A model for the optimal design and management of a cogeneration system with energy storage, *Energy and Buildings* 124 (2016) 241–247.
 - [12] A. Carravetta, G. Del Giudice, O. Fecarotta, H. M. Ramos, Pump as turbine (pat) design in water distribution network by system effectiveness, *Water* 5 (3) (2013) 1211–1225.

- [13] A. Rogeau, R. Girard, G. Kariniotakis, A generic gis-based method for small pumped hydro energy storage (phes) potential evaluation at large scale, *Applied energy* 197 (2017) 241–253.
- [14] A. Morabito, P. Hendrick, Pump as turbine applied to micro energy storage and smart water grids: A case study, *Applied energy* 241 (2019) 567–579.
- [15] G. d. O. e Silva, P. Hendrick, Pumped hydro energy storage in buildings, *Applied energy* 179 (2016) 1242–1250.
- [16] K. Kusakana, Optimal operation scheduling of grid-connected pv with ground pumped hydro storage system for cost reduction in small farming activities, *Journal of Energy Storage* 16 (2018) 133–138.
- [17] T. Ma, H. Yang, L. Lu, J. Peng, Optimal design of an autonomous solar–wind-pumped storage power supply system, *Applied Energy* 160 (2015) 728–736.
- [18] T. Ayodele, A. Ogunjuyigbe, T. Ibitoye, Optimal selection of pumped hydro storage based renewable energy generator (s) for isolated community using binary sort and search algorithm, *Renewable Energy Focus* 28 (2019) 100–111.
- [19] X. Xu, W. Hu, D. Cao, Q. Huang, C. Chen, Z. Chen, Optimized sizing of a standalone pv-wind-hydropower station with pumped-storage installation hybrid energy system, *Renewable Energy* 147 (2020) 1418–1431.
- [20] A. Stoppato, G. Cavazzini, G. Ardizzon, A. Rossetti, A pso (particle swarm optimization)-based model for the optimal management of a small pv (photovoltaic)-pump hydro energy storage in a rural dry area, *Energy* 76 (2014) 168–174.
- [21] B. S. Pali, S. Vadhera, An innovative continuous power generation system comprising of wind energy along with pumped-hydro storage and open well, *IEEE Transactions on Sustainable Energy* (2018).
- [22] B. S. Pali, S. Vadhera, A novel pumped hydro-energy storage scheme with wind energy for power generation at constant voltage in rural areas, *Renewable energy* 127 (2018) 802–810.

- [23] K. Oikonomou, M. Parvania, R. Khatami, Deliverable energy flexibility scheduling for active distribution networks, *IEEE Transactions on Smart Grid* 11 (1) (2019) 655–664.
- [24] L. W. Mays, *Water resources engineering*, John Wiley & Sons, 2010.
- [25] C. D’Ambrosio, A. Lodi, S. Martello, Piecewise linear approximation of functions of two variables in milp models, *Operations Research Letters* 38 (1) (2010) 39–46.
- [26] California ISO Open Access Same-Time Information System, [Online]. Available: <http://oasis.caiso.com> (2022).
- [27] Interdependent 33-Bus Power and 16-Node Water Distribution Test Systems with Small Pumped-Storage Hydropower, [Online]. Available: <https://usmart.ece.utah.edu/datasets/> (2022).
- [28] Modified IEEE 123-Bus Test Feeder for Intelligent Resilience Controller, [Online]. Available: <https://usmart.ece.utah.edu/123bustestsystemdata/> (2022).